A conservative Fourier pseudospectral algorithm for a coupled nonlinear Schrödinger system*

Cai Jia-Xiang(蔡加祥)[a)b)] and Wang Yu-Shun(王雨顺)[a)†]

[a)] Jiangsu Key Laboratory for NSLSCS, School of Mathematics Science, Nanjing Normal University, Nanjing 210046, China
[b)] School of Mathematics Science, Huaiyin Normal University, Huaian 223300, China

(Received 9 October 2012; revised manuscript received 6 December 2012)

We derive a new method for a coupled nonlinear Schrödinger system by using the square of first-order Fourier spectral differentiation matrix D_1 instead of traditional second-order Fourier spectral differentiation matrix D_2 to approximate the second derivative. We prove the proposed method preserves the charge and energy conservation laws exactly. In numerical tests, we display the accuracy of numerical solution and the role of the nonlinear coupling parameter in cases of soliton collisions. Numerical experiments also exhibit the excellent performance of the method in preserving the charge and energy conservation laws. These numerical results verify that the proposed method is both a charge-preserving and an energy-preserving algorithm.

Keywords: Schrödinger equation, Fourier pseudospectral method, conservation law, energy

PACS: 02.60.Cb, 02.70.Bf, 02.70.Jn, 02.70.Hm **DOI:** 10.1088/1674-1056/22/6/060207

1. Introduction

The Schrödinger system describes a wide range of physical phenomena, such as hydrodynamics, plasma physics, self-focusing in a laser pulse, and the dynamics of Bose–Einstein condensate at extremely low temperature. Here, we consider coupled nonlinear Schrödinger (CNLS) system

$$\begin{aligned} &\mathrm{i}\phi_t + \phi_{xx} + (|\phi|^2 + \beta|\psi|^2)\phi = 0, \\ &\mathrm{i}\psi_t + \psi_{xx} + (|\psi|^2 + \beta|\phi|^2)\psi = 0, \end{aligned} \tag{1}$$

where ϕ and ψ represent the complex amplitudes of two wave packets and β is a real-valued cross-phase modulation coefficient. The system was first derived by Benney and Newell[1] for two interacting nonlinear wave packets in a dispersive and conservative system. With initial condition

$$\phi(x,0) = \phi_0(x), \quad \psi(x,0) = \psi_0(x), \tag{2}$$

and periodic boundary conditions

$$\phi(x_\mathrm{L},t) = \phi(x_\mathrm{R},t), \quad \psi(x_\mathrm{L},t) = \psi(x_\mathrm{R},t), \tag{3}$$

the CNLS system admits charge conservation law

$$\mathscr{Q}(t) = \int_{x_\mathrm{L}}^{x_\mathrm{R}} [|\phi(x,t)|^2 + |\psi(x,t)|^2]\,\mathrm{d}x = \mathscr{Q}(0), \tag{4}$$

and energy conservation law

$$\mathscr{E}(t) = \int_{x_\mathrm{L}}^{x_\mathrm{R}} \left[\frac{1}{4}(|\phi|^4 + |\psi|^4) - \frac{1}{2}(|\phi_x|^2 + |\psi_x|^2) + \frac{\beta}{2}|\phi|^2|\psi|^2\right] \mathrm{d}x = \mathscr{E}(0). \tag{5}$$

The CNLS system has been studied numerically in recent years by using various methods. Wang *et al.*[2] simulated the CNLS system by using semi-explicit multisymplectic Euler-box schemes. Ismail *et al.*[3–5] respectively studied Crank–Nicolson, highly accurate and linearly implicit schemes. In Refs. [6]–[10], the authors discussed the multisymplectic midpoint schemes for the CNLS system. Ma *et al.*[11] studied the multisymplectic splitting methods for the problem. Zhang *et al.* presented the direct discontinuous Galerkin method in Ref. [12]. All methods[3–12] preserve charge conservation law exactly, however, they do not preserve the energy conservation law. In Refs. [13]–[16], some conserved charge methods and energy conservation laws are proposed for the CNLS system.

Spectral and pseudospectral methods have become very popular in the last decades because of their convergence accuracy in solving smooth problems, especially with the advent of the fast Fourier transform. Chen *et al.*[17] suggested a multisymplectic Fourier pseudospectral method to solve the CNLS by using the idea of splitting partial differential equation. But it is neither a charge-preserving nor an energy-preserving method. The aim of this paper is to construct a charge-preserving and energy-preserving Fourier pseudospectral algorithm for the CNLS system (1). We will then conduct some numerical experiments to show the performance and efficiency of the proposed algorithm.

A plan of this paper is as follows: in Section 2, a new

*Project supported by the National Natural Science Foundation of China (Grant Nos. 11201169 and 11271195), the National Basic Research Program of China (Grant No. 2010AA012304), the Natural Science Foundation of Jiangsu Education Bureau, China (Grant Nos. 10KJB110001 and 12KJB110002), and the Qing Lan Project of Jiangsu Province of China.

†Corresponding author. E-mail: thomasjeer@sohu.com or wangyushun@njnu.edu.cn

© 2013 Chinese Physical Society and IOP Publishing Ltd

scheme is proposed for the CNLS system. We prove that the method conserves the charge and energy conservation laws simultaneously. The numerical performance of the method is shown in Section 3. Section 4 is our conclusions.

2. Construction of conservative algorithm

As usual, we introduce some notations: $x_j = x_{\rm L} + jh$, $t_n = n\tau$, $j = 0,1,\ldots,N$; $n = 0,1,2,\ldots$, where $h = (x_{\rm R} - x_{\rm L})/N$ and τ are spatial and temporal step lengths. Denote u_j^n as the approximate values of $u(x_j,t_n)$ and $\boldsymbol{u} = (u_0,u_1,\ldots u_{N-1})^{\rm T}$. In order to derive the algorithms conveniently, we define $\delta_t u_j^n = (u_j^{n+1} - u_j^n)/\tau$ and $A_t u_j^n = (u_j^{n+1} + u_j^n)/2$ as difference and average operators. We also need define the inner product and p-norm ($1 < p < \infty$) of vectors as

$$\langle \boldsymbol{u}, \boldsymbol{v}\rangle = h\sum_{j=0}^{N-1} u_j \overline{v}_j, \quad \| \boldsymbol{u} \|_p = \left(h\sum_{j=0}^{N-1} |u_j|^p \right)^{1/p}.$$

As we know, the first-order differential operator ∂_x yields the Fourier differentiation matrix D_1. Here, D_1 is an $N\times N$ skew-symmetric matrix with elements

$$(D_1)_{r,s} = \begin{cases} \dfrac{1}{2}\mu(-1)^{r+s}\cot\left(\mu\dfrac{x_r - x_s}{2}\right), & r \neq s, \\ 0 & r = s, \end{cases}$$

where $r,s = 1,2,\ldots,N$ and $\mu = 2\pi/(x_{\rm R} - x_{\rm L})$. We can also obtain a Fourier spectral differentiation matrix D_2 for the second-order differential operator ∂_{xx}. For the ordinary differential equation (ODE) $u_{xx} = f$, we set $u_x = v$ and $v_x = f$. Applying the first order Fourier pseudospectral method to the two equations reads $D_1\boldsymbol{u} = \boldsymbol{v}$ and $D_1\boldsymbol{v} = \boldsymbol{f}$. Eliminating vector $\boldsymbol{v}$ gives $D_1^2\boldsymbol{u} = \boldsymbol{f}$. In this work, in order to construct a charge-preserving and energy-preserving method for the CNLS system, we use $D_1^2\boldsymbol{u}$ to approximate u_{xx} instead of $D_2\boldsymbol{u}$. This method has been used to derive multisymplectic schemes for some classical partial differential equations (PDEs).[18–22] Applying the Fourier pseudospectral method to space derivatives and the midpoint rule to the time derivatives in CNLS (1) gives

$$\begin{aligned} &{\rm i}\delta_t\phi_j^n + A_t(D_1^2\Phi^n)_j + A_t(|\phi_j^n|^2 + \beta|\psi_j^n|^2)(A_t\phi_j^n) = 0, \\ &{\rm i}\delta_t\psi_j^n + A_t(D_1^2\Psi^n)_j + A_t(|\psi_j^n|^2 + \beta|\phi_j^n|^2)(A_t\psi_j^n) = 0, \end{aligned} \quad (6)$$

where $\Phi^n = (\phi_0^n,\phi_1^n,\ldots,\phi_{N-1}^n)^{\rm T}$ and $\Psi^n = (\psi_0^n,\psi_1^n,\ldots,\psi_{N-1}^n)^{\rm T}$. Obviously, the scheme (6) can be reformed as a vector form

$$\begin{aligned} &{\rm i}\delta_t\Phi^n + A_tD_1^2\Phi^n + A_t(|\Phi^n|.^2 + \beta|\Psi^n|.^2)\cdot A_t\Phi^n = 0, \\ &{\rm i}\delta_t\Psi^n + A_tD_1^2\Psi^n + A_t(|\Psi^n|.^2 + \beta|\Phi^n|.^2)\cdot A_t\Psi^n = 0, \end{aligned} \quad (7)$$

where '$\cdot$' denotes point multiplication between vectors, that is

$$\Phi^n\cdot\Psi^n = (\phi_0^n\psi_0^n,\phi_1^n\psi_1^n,\ldots,\phi_{N-1}^n\psi_{N-1}^n)^{\rm T}.$$

In general, the charge conservation law (4), which is a quadratic invariant, plays an important part in quantum physics. Therefore, it is necessary to discuss whether the method conserves the charge conservation law exactly.

Theorem 1 With periodic boundary condition (3), the scheme (7) preserves the charge conservation law exactly, namely,

$$\mathscr{Q}^{n+1} = \mathscr{Q}^n = \cdots = \mathscr{Q}^1 = \mathscr{Q}^0, \quad (8)$$

where $\mathscr{Q}^n = \| \Phi^n \|_2^2 + \| \Psi^n \|_2^2$. The algorithm is unitary, thus the method is unditionally stable with respect to the initial value.

Proof Taking the inner product of the first line of Eq. (7) with $\Phi^{n+1} + \Phi^n$ yields

$$\begin{aligned} &{\rm i}\langle\delta_t\Phi^n, \Phi^{n+1} + \Phi^n\rangle + \langle A_tD_1^2\Phi^n, \Phi^{n+1} + \Phi^n\rangle \\ &+ \langle A_t(|\Phi^n|.^2 + \beta|\Psi^n|.^2)\cdot A_t\Phi^n, \Phi^{n+1} + \Phi^n\rangle = 0. \end{aligned} \quad (9)$$

The first term becomes

$$\begin{aligned} &\frac{\rm i}{\tau}\langle\Phi^{n+1} - \Phi^n, \Phi^{n+1} + \Phi^n\rangle \\ &= \frac{\rm i}{\tau}(\| \Phi^{n+1} \|_2^2 - \| \Phi^n \|_2^2) - \frac{2}{\tau}\Im\langle\Phi^{n+1}, \Phi^n\rangle, \end{aligned} \quad (10)$$

where $\Im$ stands for the imaginary part. The second term can be reduced to

$$\begin{aligned} &\frac{1}{2}\langle D_1^2(\Phi^{n+1} + \Phi^n), \Phi^{n+1} + \Phi^n\rangle \\ &= -\frac{1}{2}\langle D_1(\Phi^{n+1} + \Phi^n), D_1(\Phi^{n+1} + \Phi^n)\rangle \\ &= -\frac{1}{2}\| D_1(\Phi^{n+1} + \Phi^n) \|_2^2. \end{aligned} \quad (11)$$

It is a real function. The last term

$$\begin{aligned} &\langle A_t(|\Phi^n|.^2 + \beta|\Psi^n|.^2)\cdot A_t\Phi^n, \Phi^{n+1} + \Phi^n\rangle \\ &= 2h\sum_{j=0}^{N-1} A_t(|\psi_j^n|^2 + \beta|\phi_j^n|^2)(A_t\phi_j^n)(A_t\overline{\phi_j^n}) \\ &= 2h\sum_{j=0}^{N-1} A_t(|\psi_j^n|^2 + \beta|\phi_j^n|^2)|A_t\phi_j^n|^2, \end{aligned} \quad (12)$$

is also a real function. Therefore, the imaginary part of Eq. (9) implies

$$\| \Phi^{n+1} \|_2^2 = \| \Phi^n \|_2^2. \quad (13)$$

Similarly, taking the inner product of the second line of Eq. (7) with $\Psi^{n+1} + \Psi^n$, and then taking the imaginary part yields

$$\| \Psi^{n+1} \|_2^2 = \| \Psi^n \|_2^2. \quad (14)$$

Combining Eqs. (13) and (14) gives the discrete charge conservation law (9).

Remark 1 From Eqs. (13) and (14), we find that the scheme (7) also admits charge conservation laws $\| \Phi^{n+1} \|_2^2 = \| \Phi^n \|_2^2$ and $\| \Psi^{n+1} \|_2^2 = \| \Psi^n \|_2^2$.

The energy invariant (5) is also an important conservative property for the CNLS. Next, we turn our sights to study the discrete analogue of the energy conservation law.

Theorem 2 For the periodic condition (3), the scheme (7) possesses the discrete global energy conservation law

$$\mathscr{E}^{n+1} = \mathscr{E}^{n} = \ldots = \mathscr{E}^{1} = \mathscr{E}^{0}, \tag{15}$$

where

$$\begin{aligned}\mathscr{E}^{n} = {} & \frac{1}{4}(\| \Phi^{n} \|_4^4 + \| \Psi^{n} \|_4^4) - \frac{1}{2}(\| D_1\Phi^{n} \|_2^2 + \| D_1\Psi^{n} \|_2^2) \\ & + \frac{\beta}{2}h\sum_{j=0}^{N-1}|\phi_j^n|^2|\psi_j^n|^2.\end{aligned}$$

Proof Taking the inner product of the first line of Eq. (7) with $\Phi^{n+1}-\Phi^{n}$ reads

$$\begin{aligned}& \mathrm{i}\langle \delta_t\Phi^{n}, \Phi^{n+1}-\Phi^{n}\rangle + \langle A_tD_1^2\Phi^{n}, \Phi^{n+1}-\Phi^{n}\rangle \\ & + \langle A_t(|\Phi^{n}|^{.2} + \beta|\Psi^{n}|^{.2})\cdot A_t\Phi^{n}, \Phi^{n+1}-\Phi^{n}\rangle = 0. \end{aligned}\tag{16}$$

The first term

$$\mathrm{i}\langle \delta_t\Phi^{n}, \Phi^{n+1}-\Phi^{n}\rangle = \frac{\mathrm{i}}{\tau}\| \Phi^{n+1}-\Phi^{n} \|_2^2, \tag{17}$$

is a purely imaginary. The second term

$$\begin{aligned}& \langle A_tD_1^2\Phi^{n}, \Phi^{n+1}-\Phi^{n}\rangle \\ = {} & -\frac{1}{2}(\| D_1\Phi^{n+1} \|_2^2 - \| D_1\Phi^{n} \|_2^2) \\ & + \mathrm{i}\Im\langle D_1\Phi^{n+1}, D_1\Phi^{n}\rangle.\end{aligned}\tag{18}$$

The last term

$$\begin{aligned}& \langle A_t(|\Phi^{n}|^{.2} + \beta|\Psi^{n}|^{.2})\cdot A_t\Phi^{n}, \Phi^{n+1}-\Phi^{n}\rangle \\ = {} & \frac{1}{4}\Big[\| \Phi^{n+1} \|_4^4 - 2\mathrm{i}\Im\langle |\Phi^{n+1}|^{.2}\cdot\Phi^{n+1}, \Phi^{n}\rangle \\ & + \beta h\sum_{j=0}^{N-1}|\psi_j^{n+1}|^2|\phi_j^{n+1}|^2 - 2\beta\mathrm{i}\Im\langle |\Phi^{n+1}|^{.2}\cdot\Phi^{n+1}, \Phi^{n}\rangle \\ & - \beta h\sum_{j=0}^{N-1}|\psi_j^{n+1}|^2|\phi_j^{n}|^2 - 2\mathrm{i}\Im\langle |\Phi^{n}|^{.2}\cdot\Phi^{n+1}, \Phi^{n}\rangle \\ & - \| \Phi^{n} \|_4^4 + \beta h\sum_{j=0}^{N-1}|\psi_j^{n}|^2|\phi_j^{n+1}|^2 \\ & - 2\beta\mathrm{i}\Im\langle |\Phi^{n}|^{.2}\cdot\Phi^{n+1}, \Phi^{n}\rangle - \beta h\sum_{j=0}^{N-1}|\psi_j^{n}|^2|\phi_j^{n}|^2\Big].\end{aligned}\tag{19}$$

Therefore, the real part of Eq. (16) is

$$\begin{aligned}& -\frac{1}{2}(\| D_1\Phi^{n+1} \|_2^2 - \| D_1\Phi^{n} \|_2^2) \\ & + \frac{1}{4}\Big(\| \Phi^{n+1} \|_4^4 - \| \Phi^{n} \|_4^4 + \beta h\sum_{j=0}^{N-1}|\psi_j^{n+1}|^2|\phi_j^{n+1}|^2 \\ & - \beta h\sum_{j=0}^{N-1}|\psi_j^{n+1}|^2|\phi_j^{n}|^2 + \beta h\sum_{j=0}^{N-1}|\psi_j^{n}|^2|\phi_j^{n+1}|^2 \\ & - \beta h\sum_{j=0}^{N-1}|\psi_j^{n}|^2|\phi_j^{n}|^2\Big) = 0.\end{aligned}\tag{20}$$

Similarly, taking the inner product of the second line of Eq. (7) with $\Psi^{n+1}-\Psi^{n}$, and then taking its real part yields

$$\begin{aligned}& -\frac{1}{2}(\| D_1\Psi^{n+1} \|_2^2 - \| D_1\Psi^{n} \|_2^2) \\ & + \frac{1}{4}\Big(\| \Psi^{n+1} \|_4^4 - \| \Psi^{n} \|_4^4 + \beta h\sum_{j=0}^{N-1}|\phi_j^{n+1}|^2|\psi_j^{n+1}|^2 \\ & - \beta h\sum_{j=0}^{N-1}|\phi_j^{n+1}|^2|\psi_j^{n}|^2 + \beta h\sum_{j=0}^{N-1}|\phi_j^{n}|^2|\psi_j^{n+1}|^2 \\ & - \beta h\sum_{j=0}^{N-1}|\phi_j^{n}|^2|\psi_j^{n}|^2\Big) = 0.\end{aligned}\tag{21}$$

Adding Eq. (20) onto Eq. (21) gives

$$\begin{aligned}& -\frac{1}{2}(\| D_1\Phi_j^{n+1} \|_2^2 + \| D_1\Psi_j^{n+1} \|_2^2) \\ & + \frac{1}{4}(\| \Phi_j^{n+1} \|_4^4 + \| \Psi_j^{n+1} \|_4^4) + \frac{\beta}{2}h\sum_{j=0}^{N-1}|\phi_j^{n+1}|^2|\psi_j^{n+1}|^2 \\ = {} & -\frac{1}{2}(\| D_1\Phi_j^{n} \|_2^2 + \| D_1\Psi_j^{n} \|_2^2) \\ & + \frac{1}{4}(\| \Phi_j^{n} \|_4^4 + \| \Psi_j^{n} \|_4^4) + \frac{\beta}{2}h\sum_{j=0}^{N-1}|\phi_j^{n}|^2|\psi_j^{n}|^2.\end{aligned}$$

This completes the proof. □

Remark 2 It is evident that theorem 2 is consistent with the global energy conservation law (5). Therefore, the scheme (7) preserves the discrete global energy conservation law exactly.

3. Numerical experiments

In this section, we conduct some numerical experiments to show the performance of the scheme (7). The goal of the following numerical experiments includes three aspects: (i) to show the accuracy of soliton solution; (ii) to simulate the interaction of two solitons; (iii) to investigate the role of the nonlinear coupling parameter β in solitons collision; (iv) to numerically verify the method has excellent preservation of charge and energy conservation laws.

Example 1 (single solition) As we know, choosing $\beta = 1$ in the CNLS system (1) gives NLS equation

$$\mathrm{i}\phi_t + \phi_{xx} + 2|\phi|^2\phi = 0. \tag{22}$$

The equation has an analytic soliton solution $\phi(x,t) = \mathrm{sech}(x-2t)\exp(\mathrm{i}x)$. Here, we take $\phi_0(x) = \phi(x,0)$, $-20 \le x \le 60$ as the initial condition. To scale the errors of solution, we define $L_\infty(\phi) = \max_{0\le j\le N-1} | \phi(x_j, n\tau) - \phi_j^n |$. In Ref. [5], Ismail presented L_∞ errors of the linearly implicit conservative scheme (LICS) and Crank–Nicholson scheme (CNS) with $\tau = 0.01$ and $N = 800$. For the present scheme, we choose $N = 800$ and $N = 200$, respectively. Table 1 displays the errors

of solution obtained by the three schemes. It is clear that the solutions of the present scheme are much more accurate than those of the others. Further, the errors of the cases $N = 200$ and $N = 800$ are almost the same. The reason is that the error from the time discretization ($\tau = 0.01$) is not negligible comparing to those from the space approximation as N is large. The errors in charge and energy of the present scheme are shown in Fig. 1. From the figure, one can see that the errors are within the roundoff error of the machine.

Table 1. The $L_\infty(|\phi|)$ error at different times, obtained by various schemes.

Method\Time	$T = 10$	$T = 20$	$T = 30$
Present ($N = 200$)	3.37×10^{-4}	6.65×10^{-4}	9.95×10^{-4}
Present ($N = 800$)	3.35×10^{-4}	6.70×10^{-4}	9.94×10^{-4}
LICS ($N = 800$)	8.91×10^{-2}	1.88×10^{-1}	2.76×10^{-1}
CNS ($N = 800$)	3.77×10^{-2}	7.38×10^{-2}	1.09×10^{-1}

Next, we compute the problem over the region $-20 \le x \le 20$ up to $T = 1$. In order to test convergence rate in time, we take $N = 200$ and various time steps. The rate of convergence in time can be obtained by using the formula Order $= \ln(L_\infty(\tau_2)/L_\infty(\tau_1))/\ln(\tau_2/\tau_1)$. Table 2 displays the L_∞ error norms and convergence rates. From the table, one can see that the convergence rate in time is of order 2. To test the convergence in space, we choose $\tau = 0.0001$. The results in Table 3 indicate the numerical solutions converge rapidly to the accurate solutions in space, which is indicative of exponential convergence.

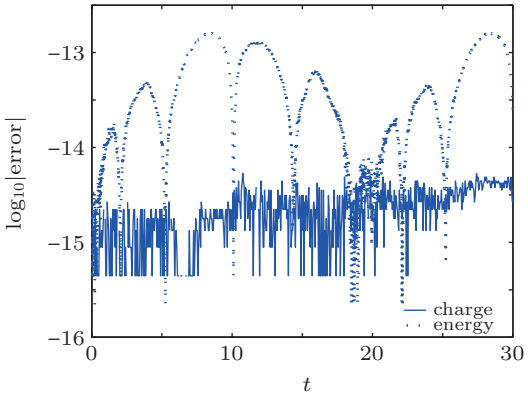


Fig. 1. (color online) The errors in charge and energy against time for a single soliton.

Table 2. The convergence rate in time, $N = 200$, $T = 1$.

τ	0.1	0.05	0.01	0.005	0.0025
$L_\infty(\|\phi\|)$	4.8656×10^{-3}	1.1957×10^{-3}	4.7484×10^{-5}	1.1868×10^{-5}	2.9669×10^{-6}
Order	–	2.0250	2.0017	2.0004	2.0000

Table 3. The maximum errors of solution $|\phi|$, $\tau = 0.0001$, $T = 1$.

N	48	64	96	128	256
L_∞	2.4569×10^{-2}	3.7312×10^{-3}	2.8259×10^{-5}	3.6231×10^{-7}	4.9927×10^{-9}

Example 2 (solitions collision) We consider the following initial condition

$$\phi(x,0) = \sqrt{2}r_1\,\mathrm{sech}(r_1x + D_0)\exp(\mathrm{i}vx/4), \quad (23)$$

$$\psi(x,0) = \sqrt{2}r_2\,\mathrm{sech}(r_2x - D_0)\exp(-\mathrm{i}vx/4), \quad (24)$$

where $-40 \le x \le 40$, $r_1 = r_2 = 1$, $D_0 = 10$, and $v = 1$. The simulations are conducted with $\tau = 0.1$ and $N = 200$ up to $T = 40$.

First, we take $\beta = 2/3$. The profiles for the numerical solutions $|\phi|$ and $|\psi|$ from beginning to the end are presented in Fig. 2. From the figure, one can see that the two solitary waves seem to be trapped after interaction. The phenomenon indicates that the collision is inelastic. Figure 3 displays the errors in invariants against time. It is clear that the errors in charge and energy are in the scale of 10^{-14}. Moreover, the errors oscillate near zeros but do not exhibit any growth for the duration of the simulation. Therefore, scheme (7) preserves the charge and energy exactly.

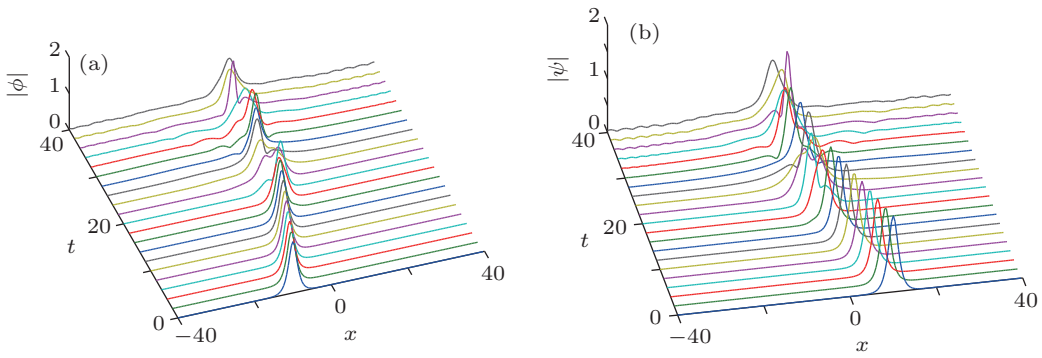


Fig. 2. (color online) Collision of two solitons for $\beta = 2/3$. (a): $|\phi|$; (b): $|\psi|$.

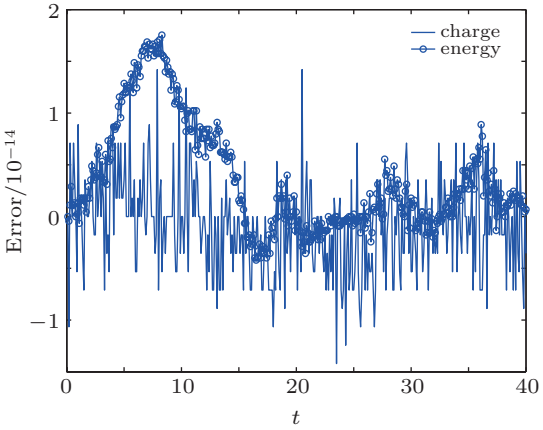


Fig. 3. (color online) The errors in invariants for the two solitons collision with $\beta = 2/3$.

Second, we discuss the case of $\beta = 2$. In such a case, two stable solitary waves, which move in opposite direction after interaction, are generated as shown in Fig. 4. Figure 5 shows the residuals of charge and energy. From the graphs, one can see that the errors in the two invariants are all in the scale of 10^{-14} throughout computations.

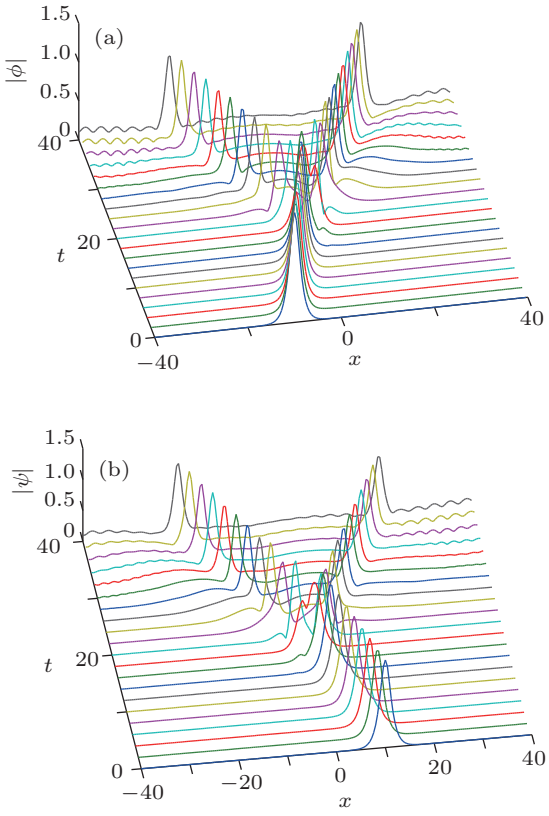


Fig. 4. (color online) Collision of two solitons for $\beta = 2$. (a): $|\phi|$; (b): $|\psi|$.

Finally, $\beta = 3$ is chosen. Figure 6 shows the evolution of the solitons $|\phi|$ and $|\psi|$ as time evolves. It is clear that three solitons appear after soliton collision. The variations of the errors in charge and energy against time are illustrated with Fig. 7. Again, the errors in the two invariants oscillate near zeros in the scale of 10^{-14}.

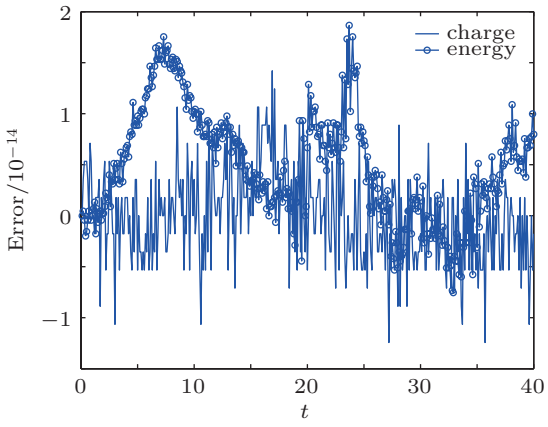


Fig. 5. (color online) The errors in invariants for the two solitons collision with $\beta = 2$.

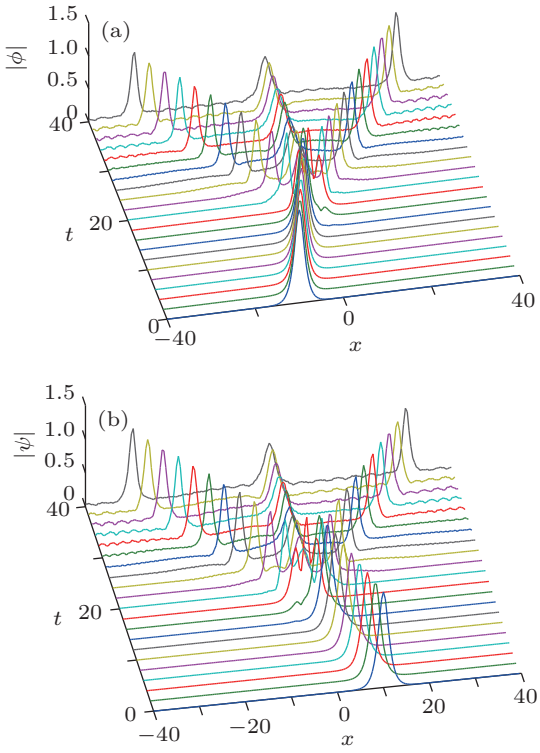


Fig. 6. (color online) Collision of two solitons for $\beta = 3$. (a): $|\phi|$; (b): $|\psi|$.

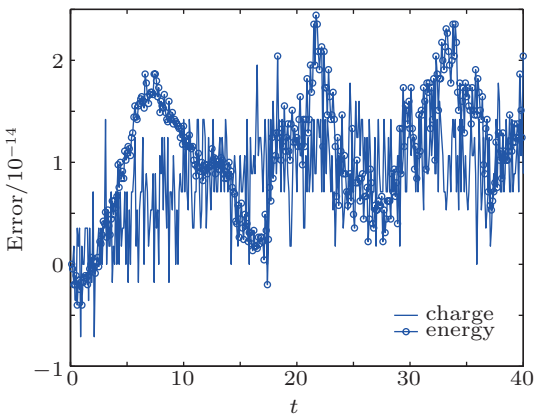


Fig. 7. (color online) The errors in invariants for the two solitons collision with $\beta = 3$.

Actually, as the value of β increases, more and more solitons will be formed after interaction. The corresponding errors in invariants are all within the roundoff error of the machine. These results are not shown here. The above numerical results verify the theoretical analysis, namely, the scheme (7) is both a charge-preserving and an energy-preserving method.

4. Conclusions

In this work, we proposed a conservative method for the CNLS equation based on applying the Fourier pseudospectral method and midpoint rule with respect to space and time derivatives. The method preserves the charge and energy conservation law exactly. The accuracy of the single soliton solution is presented. In addition, various numerical experiments were conducted to investigate the role of the nonlinear coupling parameter β in soliton collisions. Numerical experiments showed good performance of the method in preserving conservative quantities. These results verify the theoretical analysis.

References

[1] Benney D J and Newell A C 1967 *J. Math. Phys.* **46** 133
[2] Wang Y S and Li S T 2010 *Int. J. Comput. Math.* **87** 775
[3] Ismail M S and Taha T R 2001 *Math. Comput. Simul.* **56** 547
[4] Ismail M S and Alamri S Z 2004 *Int. J. Comput. Math.* **81** 333
[5] Ismail M S and Taha T R 2007 *Math. Comput. Simul.* **74** 302
[6] Sun J Q and Qin M Z 2003 *Comput. Phys. Commun.* **155** 221
[7] Sun J Q, Gu X Y and Ma Z Q 2004 *Physica D* **196** 311
[8] Sun J Q, Qin M Z, Wei H and Dong D G 2009 *Commun. Nonlinear Sci. Numer. Simul.* **14** 1259
[9] Aydın A and Karasözen B 2007 *Comput. Phys. Commun.* **177** 566
[10] Wang T C, Zhang L M and Chen F Q 2008 *Appl. Math. Comput.* **203** 413
[11] Ma Y P, Kong L H, Hong J L and Cao Y 2011 *Comput. Math. Appl.* **61** 319
[12] Zhang R P, Yu X J and Feng T 2012 *Chin. Phys. B* **21** 030202
[13] Christov C I 1994 *Phys. Scripta* **50** 449
[14] Sonnier W J and Christov C I 2005 *Math. Comput. Simul.* **69** 514
[15] Wang T C, Nie T, Zhang L M and Chen F Q 2008 *Math. Comput. Simul.* **79** 607
[16] Wang T C, Guo B L and Zhang L M 2010 *Appl. Math. Comput.* **217** 1604
[17] Chen Y M, Zhu H J and Song S H 2010 *Comput. Phys. Commun.* **181** 1231
[18] Chen J and Qin M 2001 *Electron. Trans. Numer. Anal.* **12** 193
[19] Wang J 2009 *J. Phys. A: Math. Theor.* **42** 085205
[20] Cai J X and Liang H 2012 *Chin. Phys. Lett.* **29** 080201
[21] LV Z Q, Xue M and Wang Y S 2011 *Chin. Phys. Lett.* **28** 060205
[22] Qian X, Song S H, Gao E and Li W B 2012 *Chin. Phys. B* **21** 070206